Cell Biochem Biophys (2007) 48:1–15
DOI 10.1007/s12013-007-0010-0

ORIGINAL PAPER

Exploring dynamics in living cells by tracking single particles

Valeria Levi · Enrico Gratton

Published online: 25 May 2007

Abstract In the last years, significant advances in microscopy techniques and the introduction of a novel technology to label living cells with genetically encoded fluorescent proteins revolutionized the field of Cell Biology. Our understanding on cell dynamics built from snapshots on fixed specimens has evolved thanks to our actual capability to monitor in real time the evolution of processes in living cells. Among these new tools, single particle tracking techniques were developed to observe and follow individual particles. Hence, we are starting to unravel the mechanisms driving the motion of a wide variety of cellular components ranging from organelles to protein molecules by following their way through the cell. In this review, we introduce the single particle tracking technology to new users. We briefly describe the instrumentation and explain some of the algorithms commonly used to locate and track particles. Also, we present some common tools used to analyze trajectories and illustrate with some examples the applications of single particle tracking to study dynamics in living cells.

Keywords Single particle tracking · Dynamics · Trajectory · Intracellular motion · Tracking algorithm

V. Levi
Laboratorio de Electrónica Cuántica, Departamento de Física, Universidad de Buenos Aires, Pabellón I Ciudad Universitaria, 1428 Buenos Aires, Argentina

E. Gratton (✉)
Laboratory for Fluorescence Dynamics, Rockwell Engineering Center #204, University of California at Irvine, Irvine, CA 92697-2715, USA
e-mail: egratton22@yahoo.com

Introduction

Since fluorescence microscopy started to be used to observe cells it became clear that the distribution of cellular components ranging from proteins to organelles was not homogenous in space and time. Microscopy studies on living cells also revealed that the cellular organization is highly dynamic and responds to specific stimuli. Trying to understand the rules governing such distributions has since become a priority. With this aim, microscopy techniques have been developed to measure the motion of particles and molecules in vivo.

One of the techniques widely used to quantify the motion of particles in live cells is fluorescence recovery after photobleaching (FRAP). In FRAP experiments, the molecule of interest is labeled with a fluorescent dye and introduce in the cell or expressed fused to a fluorescent protein. Then, a subregion of the cell is photobleached to create an inhomogeneity in the cellular fluorescent population and the recovery of the fluorescence intensity in the bleached region is followed as a function of time. The kinetics of this recovery depends on the speed the labeled particles move from other regions of the cell to the photobleached area [61]. A concern that is raised when using FRAP is that it requires high intensity illumination to create the photobleached region introducing undesirable effects or photodamage (see references in [35]). Also, many of the common fluorescent dyes used in FRAP do not irreversibly bleach [35, 90] complicating the interpretation of the experiments.

Fluorescence correlation spectroscopy (FCS) and related techniques scanning-FCS [64] and image correlation spectroscopy [17, 30] are becoming more

popular and hold great potential for in vivo mobility measurements (see [68] and references therein). FCS measures the fluctuations in fluorescence in the small excitation volume (~1 femtoliter) obtained in a confocal or two-photon microscope. These fluctuations are due to fluorescent-labeled molecules moving in and out of the excitation volume and depend on the average number of labeled molecules in that volume and their residence time. Fluctuation analysis-based techniques have the advantages of requiring a very low concentration of fluorescent-labeled molecules and causing minimal photodamage.

In FRAP and FCS measurements, the properties of a large number of particles are averaged. The example showed in Fig. 1 illustrates that even detecting a simple event such as binding can be extremely difficult for these large ensemble techniques. Averaging can be a problem in the complex environment of the cell since particles can interact with multiple targets resulting in populations with different mobility properties. Also, the dynamics may change in time and/or space, making the analysis of FCS and FRAP experiments more difficult.

To overcome these problems, single particle tracking (SPT) approaches were developed to follow the position of individual particles in time. Provided the spatial and temporal resolution of the method is adequate, these trajectories can be analyzed to extract quantitative information about the mechanism involved in the motion of the particle. Since every particle is observed independently, SPT can easily distinguish populations of particles with different motion properties (Fig. 1). In some complex processes, such as a virus infection, a particle can switch between different motion mechanisms. As can be observed in Fig. 2, the trajectories of the particles are signatures of the mechanism responsible for the motion in each stage showing that SPT is also an important tool to explore complex processes. These characteristics make SPT an appealing technique to achieve the ultimate goal of understanding dynamics in cells.

This review is intended to introduce single particle tracking to potential, new users. First, we present an overview of single particle trajectories analysis. Next, we briefly describe the instrumentation of single particle techniques and the probes used to label the target particles. Then, we discuss some of the algorithms used to locate and follow individual particles. Finally, we illustrate with some examples the applications of single particle tracking to study dynamics in living cells.

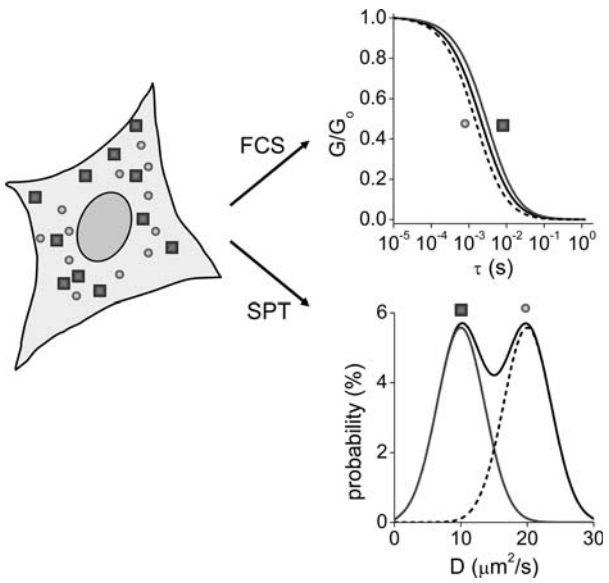

Fig. 1 Measurements of diffusion by SPT and FCS. Small, fluorescent particles (grey circles) passively diffusing in a cell cytoplasm associate reversibly with a cellular target resulting in a complex of increased mass (black squares) but same brightness (left panel). FCS and SPT measurements on this cell (top-right and bottom-right panels, respectively) were simulated considering the same populations of free particles and complexes and diffusion coefficients of 10 and 20 μm^2/s, respectively. G/Go is the relative autocorrelation calculated as described before [6]

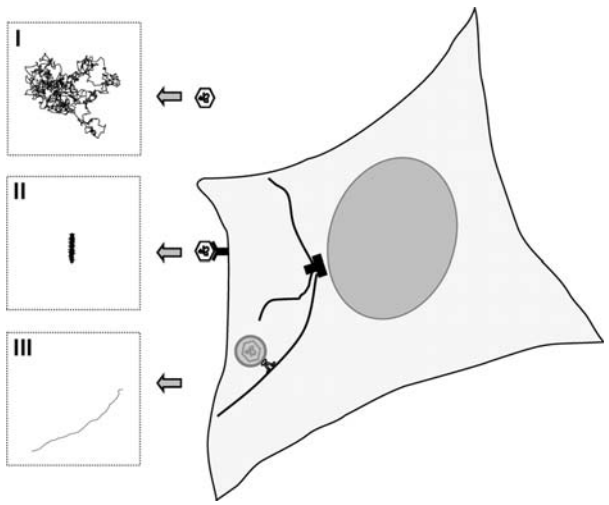

Fig. 2 Dissecting a complex cellular process with SPT. A virus particle passively diffusing in the extracellular medium (I), binds to a receptor on the plasma membrane of a cell, restricting the motion to diffusion within the membrane (II). The particle enters the cell through endocytosis and the endosome moves in the cell cytoplasm along microtubules with the aid of molecular motors (III). Trajectories obtained by sumulation are represented in the right panels. These stages are observed during some viral infections [81]

Analysis of single particle trajectories

In this section, we describe some general rules applicable to single particle trajectories analysis and methods to derive a possible model of motion from this analysis.

In order to interpret the data properly, it is extremely important to have statistically enough number of trajectories. A visual examination of isolated segments of any trajectory would suggest different mechanisms of motion since there is always a non-zero probability of observing a given path in every trajectory. For example, the trajectory obtained by simulating a virus moving randomly in the extracellular medium (panel I in Fig. 2) suggests periods of active transport; motion restricted to a small volume and unrestricted random motion.

The initial, most common approach to analyze single particle trajectories is to calculate the mean square displacement (MSD) as follows:

$$\mathrm{MSD}(\tau) = \left\langle (x(t)-x(t+\tau))^2+(y(t)-y(t+\tau))^2+(z(t)-z(t+\tau))^2 \right\rangle \quad (1)$$

where x, y, and z are the coordinates of the particle, τ is a lag time and the brackets represents the time average.

Figure 3(A) shows an example of the MSD calculation for a one-dimension trajectory. As can be observed in the figure, the calculation of MSD at longer τ is done with less data. Then, these values have a lower statistical significance than those obtained at shorter τ. A common criterion when calculating MSD is to restrict the analysis to τ values lower than 1/4 of the total time of the trajectory [69].

MSD indicates how far a particle traveled after a time lag thus; its dependence with τ is related to the motion properties of the particle. Consequently, a possible mechanism for the particle motion can be obtained by comparing the experimental MSD plot with predictions from different motion models.

Different authors [60, 69–75] derived theoretical expressions for the dependence of the MSD with τ for particles moving under different mechanisms. As examples, the following equations consider normal random diffusion (Eq. 2), anomalous subdiffusion (Eq. 3), and directed motion with diffusion (Eq. 4) in 3 dimensions.

$$\mathrm{MSD}(\tau) = 6D\ \tau \quad (2)$$

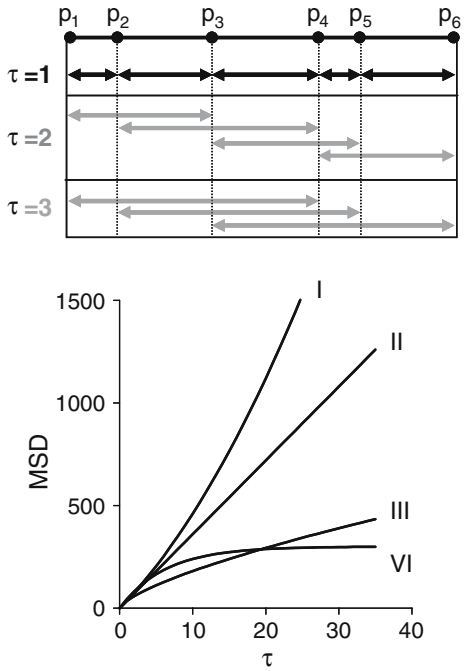

Fig. 3 Mean square displacement analysis. (**A**) MSD calculation in a one-dimensional trajectory. (**B**) Expected MSD curves for active transport (I), random diffusion (II), anomalous diffusion (III) and confined diffusion (VI). τ and MSD in arbitrary units

$$\mathrm{MSD}(\tau) = 6D\ \tau^{\alpha} \quad (3)$$

$$\mathrm{MSD}(\tau) = 6D\ \tau + (v\tau)^2 \quad (4)$$

where D and v are the diffusion coefficient and velocity of the particle, respectively and α is a coefficient <1. The anomalous subdiffusion model considers the presence of potential energy traps, e.g. other components of the cell interior that interacts with the diffusing particle slowing it down [20]. We refer the readers to the references mentioned in Saxton and Jacobson [69] for the derivations of the equations.

Figure 3(B) shows the MSD versus τ plots expected for particles moving according to these simple models. The figure also includes the MSD behavior observed for a particle diffusing randomly within a confined volume or corral. At low values of τ, the particle moves distances shorter than the limits of the corral hence the plot is approximately linear; at long lags, MSD reaches a maximum value which is related to the size and shape of the corral. The exact shape of the MSD versus τ curve depends on the geometry of the corral, some equations were derived considering simple geometries such as a circle, a rectangle or a hexagon [75].

The trajectories analysis can be done either by fitting one-by-one the MSD plots obtained for individual particles or by fitting a MSD versus τ curve calculated as the average of the plots of several particles. While the latter option is similar to averaging in ensemble measurements, the first procedure provides the distribution of motion parameters such as diffusion coefficients and velocities. These distributions can be useful to detect different populations of particles as shown in Fig. 1.

Sometimes, changes on the motion mechanism can be suspected by visual examination of the trajectories. In this case, the trajectories can be divided in two or more fragments according to the suspected transition and the MSD analysis done independently in each of the parts. Such an analysis over a large number of trajectories could help to determine quantitatively if there was a switch in the particle motion, the dynamics of the particle before and after the switch, and the time the particle spent in each motion mode. By using this approach, Lakadamyali et al. [40] dissected three individual stages during the influenza virus infection. First, the virus moves slowly in the cell periphery, then it travels rapidly toward the nucleus and once it reaches the perinuclear region, it starts moving intermittently and bidirectional until it fuses with an endosome. The MSD plots obtained in the different stages show that during the three stages the virus is actively transported, but at different velocities. By doing SPT experiments in cells in which actin filaments or microtubules were depolymerized by drugs, they could determined that the virus moves along actin filaments during the first stage while in the second and third stage, it moves along microtubules. These results allowed the authors to propose a model for the infection pathway in living cells.

Instrumentation

Microscope setup

Particle tracking techniques requires special care when selecting the microscope setup. Since in most SPT techniques the sample is illuminated several times to obtain an adequate description of the particles dynamics, cell photodamage can be a limitation factor. Hence, it is very important to minimize the time of exposure and the intensity of illumination by selecting imaging optics with high transmission efficiency and sensitive detectors that can work at low light levels.

When tracking molecules labeled with dim probes such as single dyes, the cell autofluorescence could constitute a serious problem for widefield microscopies since the signal-to-noise relation (S/N) is low. In those cases an efficient reduction of background fluorescence is required and confocal [83], multiphoton [80], or total internal reflection [76, 95] setups are preferred.

Cameras

Most of the methods used to follow the motion of particles are based on recording images of a sample field including the particle of interest as a function of time. This movie is afterwards analyzed as described in the next section to recover frame-by-frame the particle position. As the movie is recorded at a given focal plane, this analysis only provides information about the motion of the particle within that plane. In this section, we described the advantages and disadvantages of some cameras for the specific application of single particle tracking. Further details on cameras, including the basic principles and applications, can be found elsewhere [7, 57, 82].

When selecting a camera, two major points should be considered. It should be sensitive enough to detect the target particle and fast enough to detect the details of the particle motion. In cases in which the sensitivity is the important factor, the camera of election is a cooled or intensified back illuminated CCD (charge coupled device) camera.

In the cooled CCD camera the temperature of the detector is reduced to about –30°C by using a thermoelectric cooler [57] thus decreasing the dark noise. Hence, these cameras are able to detect dim particles such as single fluorophores if the exposure time is sufficiently long [3]. In this case, they are operated at low speed (~10 frames/s) therefore they can only be used to detect slow particles.

The intensified CCD cameras use an image intensifier coupled to a CCD camera, which multiplies the incoming photons that are subsequently detected by a traditional CCD chip [57]. These cameras have higher sensitivity and can be operated at relatively higher speeds than cooled-devices.

Recently, it has been introduce the on-chip multiplication gain technology, which improved the speed of cooled-CCDs. In a regular CCD camera, the output of the readout amplifier is further multiplied, process in which both the signal and the readout noise increase to the same extend. In on-chip multiplication gain devices; the CCD possesses a multiplication register that acts in a similar way of the dynodes arrangement in a photomultiplier tube. Before reading the

photon-generated charge in each pixel directly, the electrons are first accelerated from pixel to pixel in the multiplication register. Secondary electrons are generated in this process resulting in a multiplication of the initial charge. By using this technology, the camera can reach speeds higher than 1000 frames/s with very good sensitivity and very low readout noise [56].

When light is not a limitation, other less expensive, low-sensitivity cameras can be used. For example, Kusumi et al. [39] used a CMOs camera to follow the motion of lipid bound to gold nanoparticles reaching speeds of 40,000 frames/s.

Probes

Different probes have been used in particle tracking, from latex fluorescent microspheres with sizes in the range 20–1000 nm [43], colloidal gold with a diameter of 40 nm [39], 5–10 nm diameter quantum dots [14], and multiple or single copies of fluorescent molecules, with sizes of a couple nanometers [5, 99]. While bigger probes tend to be easier to follow, they slow down the studied particle and, more important they may affect the normal interactions of the particle within the cell. For example, Meier et al. [51] attached 500 nm beads to the glycine receptor to study its diffusional behavior in the membrane of living neurons. Given the big size of this probe, the labeled receptor was unable to access synaptic locations. Dahan et al. [14] overcame this limitation by using quantum dots. Since the diameter of the probe was nearly 2 orders smaller than that of the beads previously used, the labeled receptor could access synaptic locations. This experimental approach allowed a complete characterization of the mobility of the receptor in synaptic, perisynaptic, and extrasynaptic locations.

Fluorescent beads are commonly used in particle tracking because they are brighter than single dye molecules. These beads are loaded with an equivalent of unquenched fluorescent dyes ranging from 200 to 10^{10} copies of the dye for microspheres of 20 nm-15 μm diameter [29]. Hence, they provide higher S/N ratio and can be tracked with regular microscope setups for longer periods than single dyes.

Quantum dots (QD] are an interesting and yet not fully exploited option for particle tracking. The molar extinction coefficients of these nanocrystals are about 10–50 times larger than those of organic dyes and they have been found to be 10– 20 times brighter than organic dyes (see references in [9, 22]), QDs are thousand times more stable against photobleaching than organic dyes being well-suited for long and continuous tracking studies sometimes, over hours [18]. Another important characteristic of these nanoparticles is that they can be excited in a wide spectral window, from the UV to the red. The maximum of the emission band depends on the size of the quantum dot core, so they can be ''tuned'' at the desired wavelength. Also, the emission band is very narrow so the emissions of different QDs can be easily separated by an adequate but simple microscope setup. This advantage made it possible to study the stepping of the myosin-V motor along actin filaments by tracking in vitro the myosin heads labeled with QDs of different colors [94]. If we would like to do the same two-color tracking experiments with particles labeled with organic dyes, we would need a couple with a similar excitation band and not overlapping emissions, which is difficult to achieve.

So far, a limitation of QDs is the random intermittence of their fluorescent emission or blinking [37]. This fact shortens the time they can be tracked but on the other hand it provides evidence that the trajectory corresponds to a single particle since only single QDs blinks.

Several approaches have been followed to attach quantum dots and microspheres to the particle of interest (for references, see [29, 52]). The easiest and most common strategies consist on modifying the surface of the QD or microsphere with an adapter protein (e.g., streptavidin, protein A, a secondary antibody) that facilitates the binding to the target molecule. The main disadvantage of this approach is that it increases even more the size of the complex. Direct binding of the particle to the QD or microsphere through a chemical linker generally results in smaller particles but it is a time-consuming approach.

Another alternative of probes are single fluorescent dyes. They have smaller sizes than the probes previously mentioned and generally do not affect significantly the properties of the target particle. They are dimmer that QDs or microspheres and photobleach, reducing the tracking temporal window to seconds [67] and making it necessary to use relatively more sophisticated microscope systems and very sensitive detectors.

Gene-encoding fluorescent proteins have been also successfully used for single particle tracking (see for example [66]). As mentioned above, these proteins revolutionized the way we study living cells since they can be expressed fused to the target protein avoiding the problems of doing a chemical modification of the target particle and disrupting the cell to incorporate the labeled particles.

Non-fluorescent probes have also been successfully employed in single particle experiments. Generally,

they need to be big enough to be observed using brightfield microscopy. In some cases, the S/N ratio can be improved by using contrast generation techniques such as difference interference contrast [25].

Examples of these probes are colloidal gold nanoparticles of diameters in the range of 50 nm that can be detected because they scatter light out of the objective aperture [24]. Since they do not present bleaching as fluorescent probes, they can be observed for longer periods. The uses of these nanoparticles for in vivo particle tracking experiments started with the earlier works of Sheetz et al. [77] and Brabander et al. [8] who studied the lateral diffusion of membrane glycoproteins. The group of Kusumi studied the plasma membrane organization using lipids or membrane proteins labeled with 40 nm colloidal gold particles (see references in [39]). The big size of these particles allowed them to obtain a high S/N relation and pushed the limits of the temporal resolution to about 25 μs.

Locating particles with high precision

The first step of every tracking routine is to locate the particle with high precision. Considering that the size of cells ranged from 10 to 100 μm [1], the particle coordinates have to be recovered with a precision better than ~100 nm, depending on the specific application.

A point-like particle forms a diffraction-limited image of width approximately equal to $\lambda/(2\mathrm{NA})$, where λ is the wavelength of the light and NA is the numerical aperture of the objective. For visible light, this equation implies that the image of this particle has a diameter of ~200 nm. According to this, it would be impossible to locate the particle with the precision required for studies in living cells.

Several approaches have been followed to overcome this limit. All of them are based on the fact that the image of a punctual particle is not homogeneous: it follows a spatial pattern named point spread function (PSF). Then, the particle position can be recovered with high precision using a deconvolution technique in which the particle image is fitted with a theoretical distribution function. For fluorescent single molecules the PSF can be well approximated to a Gaussian function with the center corresponding to the position of the particle. Using this approximation, Yildiz et al. [99–101] located molecular motors labeled with single fluorophores with an error of 1.5 nm.

Another approach used to locate particles is the centroid method in which the position of the center of mass of the particle (x_{CM}, y_{CM}) is calculated as follows [11]:

$$x_{\mathrm{CM}} = \frac{\sum_{i=0}^{w}\sum_{j=0}^{h} i \times I(i,j)}{\sum_{i=0}^{w}\sum_{j=0}^{h} I(i,j)},\quad y_{\mathrm{CM}} = \frac{\sum_{i=0}^{w}\sum_{j=0}^{h} j \times I(i,j)}{\sum_{i=0}^{w}\sum_{j=0}^{h} I(i,j)} \tag{5}$$

where $I(i,j)$ is the intensity at the pixel located at (i,j) of an image of dimensions $w \times h$ pixels^2.

This method has the advantage of not requiring the assumption of a theoretical description of the intensity distribution. Thus, it can be used to locate big and even asymmetric particles. The method is faster than fitting a Gaussian or other theoretical function to the intensity distribution as no fitting is required.

The main problem of centroid calculation is that it is vital to exclude as much background as possible since this would strongly bias the calculation of the center of mass [12]. This is critical when the intensity of the background is not homogeneous as it is usually observed in cell measurements.

Tracking algorithms for image stacks analysis

The most common procedure to obtain trajectories of particles consists on recording a movie of the particle of interest and recovering its position by using any of the tracking algorithms described below. These methods were extensively discussed by Carter et al. [11] and Cheezum et al. [12]; some of them are schematized in Fig. 4.

As we discussed in the previous section, the particle coordinates can be obtained by either fitting a Gaussian distribution function to its intensity profile or by center of mass calculation. Repeating this procedure frame-by-frame allows the determination of the trajectory of the particle.

In correlation methods [25], an intensity pattern containing the complete description of the intensity distribution of the particle is recorded in the first frame of the sequence. The pattern is then overlaid to the following frame and shifted in one-pixel increments. A correlation value scores how well the intensity of the shifted pattern matches the intensity of the analyzed region of the image, at every pixel. The particle position is then found at the maximum in the correlation matrix. By following this procedure, we can only determine the position of the particle with an error of a pixel whose length is usually in the order of 30–150 nm. To have sub-pixel resolution, a region of the correlation matrix including the pixel where the maximum

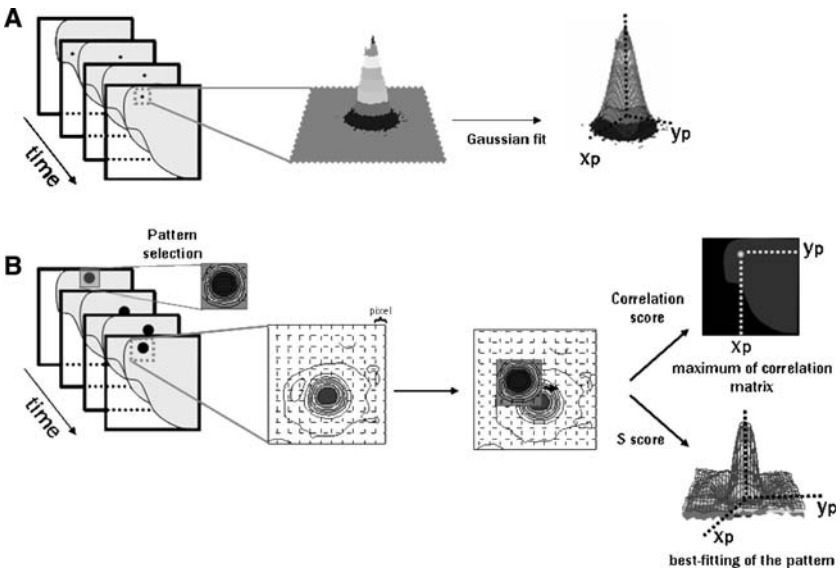

Fig. 4 Determination of particle trajectories from an image stack. (**A**) The image of a punctual particle moving in a cell produces an intensity profile that can be fitted with a Gaussian distribution function to obtain the particle position. (**B**) Correlation and pattern recognition approaches register a pattern of the particle intensity from the first frame of the movie. To calculate the position of the particle in the next frames, the pattern is moved pixel by pixel to obtained the maximum of the correlation matrix or the minimum S value, respectively

was observed and its four nearest neighbors in the x and y direction is interpolated with a paraboloid, Gaussian, or cosinusiod equations [12].

The main disadvantage of this approach is that it tends to match the brightest regions of two images rather than the best topographical fit. This can lead to severe errors, moreover in cases in which other structures different from the particle to track are observed in the frame [12].

To overcome this limitation, we developed a new pattern-recognition tracking method that combines the advantages of the Gaussian fitting and correlation approaches [44, 45]. In this method, we select a pattern from the first frame of the movie containing the image of the particle. Since this pattern is pixilated, the routine first smooth it by performing a bilinear interpolation between adjacent pixels obtaining a smoothed pattern that is used in the following frames to determine the particle position. In the next frame, the pattern is shifted around the position determined for the particle in the previous frame and a parameter S that scores the absolute intensity differences between image and pattern is calculated for the different pattern positions. In comparison to correlation methods, the S value is going to be minimal only if the image in the frame matches the pattern features, thus it can identify the particle of interest from other structures present in the frame. Another advantage is that the method does not need a theoretical expression for the intensity distribution of the particle as Gaussian fitting methods. The particle position is calculated with sub-pixel resolution by determining the position corresponding to the minimum value of S with a parabolic interpolation. By using this method, we could recover the position of 500 nm particles with 2 nm precision and 10 ms temporal resolution.

Precision on the particle position determination

Thompson et al. [85] derived the following approximated equation that can help us to understand the factors limiting the precision on the determination of the position of a single fluorescent dye using a Gaussian pattern:

$$\left\langle (\Delta x)^2 \right\rangle = \frac{s^2}{N} + \frac{a^2}{12N} + \frac{8\pi s^4 b^2}{a^2 N^2} \tag{6}$$

where Δx is the error in the particle position in one dimension, s is the standard deviation of the PSF, a is the pixel length, N is the number of photons collected and b is the background noise.

The first term arises from the photon noise, which results from the fact that the photon emission is a random process that obeys a Poisson distribution, thus, this error represents the fluctuations in the number of photons collected in a given temporal window. The second term is the pixelation noise and is due to the finite size of the pixels. This noise arises from the uncertainty on where the photon arrived in the pixel and thus increases the apparent size of the image spot. The last term is related to the background noise and represents the error introduced on the position determination by photons coming from sources different from the particle. Common sources of background noise include readout error, dark current noise, and, in the case of cells, autofluorescence.

A qualitative examination of this equation helps us to understand several aspects related to the precision on the particle position determination.

The inverse dependence of the error on the number of collected photons shows that brightfield strategies are often more precise than fluorescence techniques. However, these techniques usually require several folds larger probes than fluorescence microscopy.

The pixel size is also an important factor on the position precision. If it is too big, the pixelization error is dominant but making it small does not help too much since the signal decreases compared to the background as a result of spreading the image over a larger number of pixels, thus the third term of the equation dominates. Thompson et al. [85] demonstrated that in practice, the pixel size should be around the standard deviation of the PSF.

The equation presents two limits for the resolution: in the case of bright particles, the resolution is determined by photon counting noise, while the error on the position of dim particles is going to be limited by the background noise.

Tracking algorithm for confocal and two-photon microscopy

If we would like to track particles by recording an image stack in a confocal or a two-photon microscope, the speed of the tracking is going to be limited by the time the laser takes to scan the area of interest. In most common setups the image acquisition rate is in the order of 1 frame/s and therefore could only be used to track slow particles.

A completely different approach to the image stacks methods described above was followed by our group [34, 42, 43] based in the early theoretical work of Enderlein [19]. We designed a technique to track particles in 3-dimensions for confocal or two-photon microscope setups with a temporal resolution of 32 ms.

During a cycle of the tracking routine, the excitation laser traces a given number of small circles (of radius equal to the PSF waist) surrounding the particle to track. To track in 3-dimensions, the circles are done in two z-planes above and below the particle; the axial position is adjusted by moving the objective with a piezoelectric-nanopositioner.

The dependence on the intensity profile with the particle position for this cycle of tracking was mathematically derived [34] providing a way to determine the (x, y, z) coordinates of the particle. Figure 5 represents the fluorescent profile expected during 2 cycles of the tracking when the particle is slightly shifted with respect to the center of scanning. In the tracking routine, the determination of the particle position is done on the fly by analyzing the fast Fourier transforms of the intensity signal. Before the next cycle of tracking, the center of scanning is moved to the position determined for the particle in the previous cycle. Thus, the laser follows the particle and the trajectory is obtained in real time.

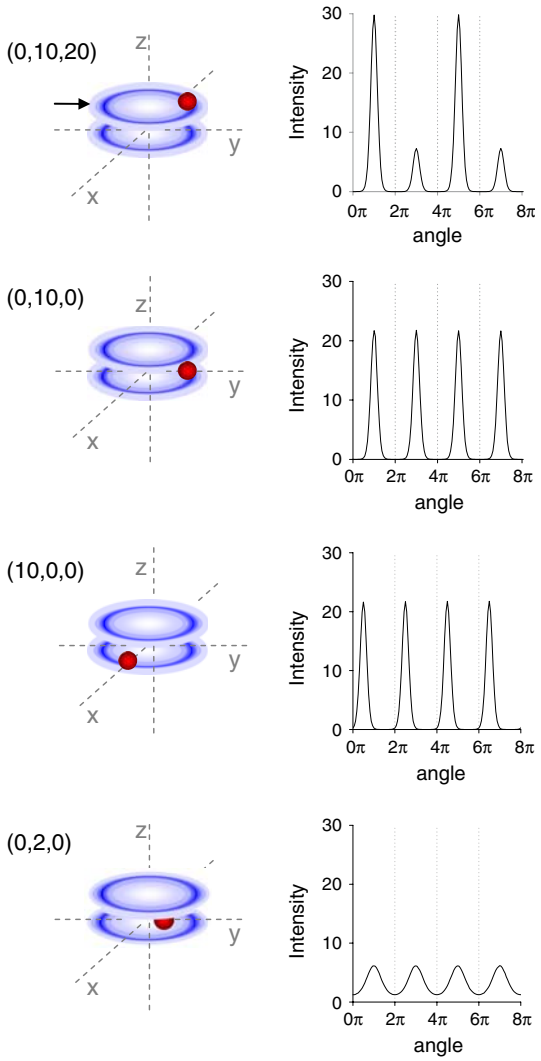

Fig. 5 Determination of the particle position in a two-photon microscope. The intensity profile determined along two cycles of the tracking routine is represented as function of the angle of rotation of the laser, for different relative positions of the particle with respect to the center of scanning (right panels). In the examples, each cycle of the tracking routine consisted in two orbits, each one at a different z-plane. The left panels show diagrams of the relative position of the particle (black circle) respect to the center of scanning. The laser orbits are represented with ovals. The arrow shows the starting point of the tracking cycle

The theoretical accuracy of the tracking routine, calculated by tracking a simulated particle with diffusion coefficient equal to zero, is ~1 nm for the x and y axis and ~3 nm for the z axis. The difference between the accuracy on the lateral (x, y) and axial (z) positions is due to the fact that the x, y-waist of the PSF is about three times smaller.

In a recent article [43], we performed control experiments—tracking fluorescent microspheres moving in known paths—in which we demonstrated that the method can recover trajectories up to 10 μm with 20-nm precision and a time resolution of 32 ms. Also, we showed that the error of the position determination is inversely proportional to the square of the S/N ratio, as it was predicted [34] being approximately constant for S/N > 2. The theoretical limit cannot be reached experimentally probably due to instrumental factors such as thermal and mechanical jitter that contribute to the noise of the measurements.

The tracking routine can also be used to track 2 particles even if they are at different axial positions. The initial coordinates for the particles are set by selecting them interactively from the fluorescence image computer display. The tracking routine starts on top of one of the particles; after a given number of cycles, the laser jumps to the position of the second particle where it performs the same routine for tracking. Then, the center of scanning is moved to the position determined previously for the first particle, thus the positions of the particles are recovered alternately.

We consider that the technique could be of great potential for the study of dynamics of fluorescently tagged particles in biological systems since two-photon microscopy provides significantly lower out-of-focus photodamage and photobleaching than other fluorescence microscopies [58]. Also, during the tracking we focus the laser in a small volume surrounding the particle, minimizing the photodamage of the rest of the sample. In contrast, methods that employ video cameras require repetitive exposures of large sample volumes that could result in significant damage.

Background noise

When doing particle-tracking experiments in cells, the background noise –due to the detection of other compounds different from the particle of interest- is usually a limit to the accuracy of the tracking. Thus, it is important to compare how the algorithm used for the tracking depends on the background noise.

Equation 6 predicts that the position of a particle obtained by Gaussian fitting depends sensitively on the intensity of the background. Figure 6 shows that the uncertainty on the particle position abruptly increases by adding a background representing a small percentage of the total counts. Thus, we should be extremely careful when using this method in cell measurements and only restrict its application to cases in which the brightness of the particle is high. In contrast, the precision on the particle position determination using the tracking routine based on the circular scanning is approximately constant with the background intensity in a wide range (Fig. 6). This is due to the fact that the FFT of the intensity signal is not affected by a locally homogeneous background noise.

Examples of innovative applications of SPT in cell biophysics

Membrane organization and function

The textbook image of biological membranes based on the fluid mosaic model proposed by Singer and Nicolson [79] has been demonstrated to be an oversimplification of the plasma membrane structure [46]. Single particle tracking constituted a very important technique to understand some aspects of the organization of cellular membranes since it provided the tool to

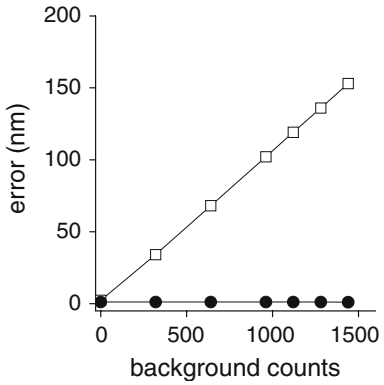

Fig. 6 Dependence of the precision on the particle position determination with the background noise. The error for the circular scanning routine (black circles) was calculated as the standard deviation of the position recovered for a simulated fixed particle after 1000 cycles of tracking in two dimensions. The background counts are the average number of counts measured during each cycle of the tracking routine in the absence of the particle. The background noise was assumed to have a Poissonian distribution. The error for the Gaussian-fitting routine (white squares) was calculated from Eq. 6. In both cases it was assumed that the photons detected from the particle were 12,000, either during one cycle of the circular-scanning routine or in one frame of the Gaussian-fitting routine. The pixel size and waist of the point spread function were 250 nm

observe the motion of lipids and proteins in situ. By using this approach, different authors could verify that the motion of membrane components is not random as it would be expected according to the Singer and Nicolson model.

By recording trajectories of lipid molecules [21, 54] and membrane proteins [65, 86], different authors observed that the motion of both components in natural membranes is highly restricted. Several works from the group of Kusumi (see references in [39]) described this motion as ''hop diffusion'' i.e., the protein or the lipid diffuses freely within a compartment until it shifts to another compartment. This behavior seems to be a consequence of steric hindrance between the cytoplasmic domains of protein with the cytoskeleton meshwork in close proximity to the bilayer [62, 86]. In the case of small lipid molecules, the restriction seems to arise from the presence of membrane proteins anchored to the actin filaments directly in contact with the membrane, which act as rows of pickets that temporarily confine lipids [21]. This model explains satisfactorily the behavior of some membrane components in some cell types. However, its generalization may not be straightforward and other mechanisms should also be taken into account [10, 78]. In particular, it has been shown that the diffusional properties of membrane proteins could change with the structural/biological state of the protein [47], adding a higher level of complexity to the membrane structure and function.

Molecular motors

Molecular motors are proteins that use energy provided from ATP hydrolysis to exert a mechanical work. Examples of such proteins are kinesins, myosins and dyneins that transport cargo along cytoskeleton tracks (see [92] and references therein). Motors proteins are essential to achieve a dynamical organization of the cytoplasm. Also, several pathogens exploit the cytoskeleton-based transport system to travel in the cell interior and reach their cellular target [2].

In this section, we briefly described some quantitative single particle tracking experiments that reveal important aspects of the function of motors in isolated systems and living cells.

Motor stepping

The common core structure of most motors proteins consists on two motor domains connected by a stalk to a globular tail, which binds to the cargo. These domains attach to the microtubules in a coordinate manner and undergo conformational changes driven by ATP hydrolysis, which propel the motor molecule (for recent reviews, see [92, 97]). The group of Selvin [99–101] followed the motion of isolated motors labeled with a single fluorescent probe in one of the heads therefore, they could discriminate the motion of a single head from the other during each motor step, impossible to do using other techniques such as optical trapping. They found that the distance traveled by the fluorescent head was twice the step size of the motor when the probe was near the motor domain. This result was compatible with a ''hand over hand'' mechanism in which both heads alternates in the lead during consecutive steps. Increasingly detailed information regarding the stepping mechanism, including the structural changes of the motor, could also be obtained by more sophisticated SPT techniques that measure the probe angular orientation during the stepping (see for example [84, 87]).

The improvement of the spatial and temporal resolutions of SPT methods allowed the detection of single steps of organelles transported by motors in cells [38, 45]. Surprisingly, the steps of pigment organelles driven by myosin V were slower than what it would be expected according to transport measurements in aqueous solution [45] also showing the differences between in vitro and in vivo transport experiments.

Coordination between motors with different polarity

Most cargoes in the cell cytoplasm are transported bidirectionally due to the presence of kinesin and dynein motors, which move toward the plus and minus end of the microtubule, respectively (for recent reviews, see [28, 97]). Different models have been proposed to explain how the final destination of an organelle is determined in the presence of motors of opposite polarities. The first model considers that only one type of motor can be bound to the cargo at any time thus, reversals are a consequence of switching the motor that is bound to the cargo. This model was ruled out in experiments in which enhanced green fluorescence protein (EGFP) labeled dynein attached to an organelle was found to move bidirectionally with the organelle [48]. Also, isolated organelles did not require any cytoplasmic component to move bidirectionally in vitro [63]. The tug of war model—in which both motors compete with each other and the final direction of the organelle is given by the motor that for some reason can exert more force- was discarded since tracking experiments showed that impairing the function of one of the microtubule motor did not improved

the transport driven by the motor of opposite polarity [26, 27]. From these results, it was concluded that both motors are coordinated during the transport. Some of the mechanisms that determine which motor is active are beginning to be understood [16].

Transport driven by multiple copies of motors

The velocities of organelles moving either toward the plus or the minus end of microtubules showed a quantized distribution with peaks located at multiple values of a basal velocity. This result was interpreted considering that multiple copies of motors are required to transport organelles in vivo [33, 38, 44, 96]. In contrast, only one copy of processive motors is usually enough to carry a big bead in vitro, pointing out the importance of in vivo transport experiments to understand the function and regulation of motor proteins. In the case of pigment-organelles transport driven by cytoplasmic dynein, the velocity distribution presents a higher contribution of high-velocity peaks after activation of the motor, showing that the change in the number of active copies of the motor constitutes a regulatory mechanism to speed up or slow down the cargo [44].

Organization and dynamics of the nucleus

Recent works have shown that the nucleus is not a homogeneous organelle but is spatially and temporary organized [53]. Finding out how this organization is achieved and how nuclear processes depend on it is critical to our understanding of nuclear function. SPT is an important tool to explore the dynamics of some of the nuclear components. In this section we briefly described some SPT studies that improved our understanding of chromatin, Cajal, and promyelocytic leukemia (PML) bodies dynamics.

Chromatin

To follow the motion of DNA during the cell life, Belmont and coworkers developed a method to label small DNA regions in live cells, which consist on the insertion of lac operator repeats in the DNA and the expression of the lac repressor protein fused to EGFP [4, 5]. These inserts are visualized as bright dots in fluorescence images of live nuclei. Consequently, they can be tracked by using any of the methods previously described.

SPT studies in different cell lines [13, 49, 93] have described the motion of these labeled chromatin regions as Brownian motion limited to a nuclear sub-

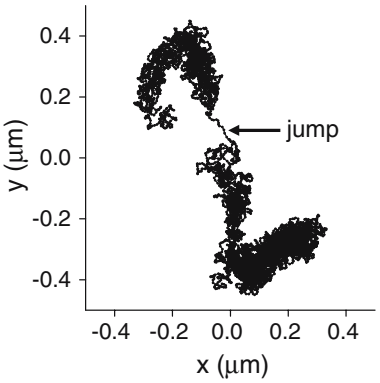

Fig. 7 Chromatin dynamics in a cell nucleus. The trajectory of an EGFP-labeled chromatin sequence was obtained by the two-photon microscopy SPT method described in the text with a time resolution of 32 ms. A region of curvilinear motion is shown with an arrow. Reprinted with permission from [42], copyright Biophysical Society, 2005

region. However, the dynamics of chromatin seems to be more complex. Heun et al. [32] reported changes in the mobility during the cell cycle and found that the movement in G1 phase was highly sensitive to ATP depletion and to changes in metabolic status. Also, changes in transcriptional activity of certain genes have been shown to be correlated with changes in their intranuclear location [91]. These results suggest that important nuclear functions such as DNA transcription are accompanied with defined changes in the position of the sequence. However, there is little experimental support to date for an active mechanism driving these chromatin movements [23].

We reexamined interphase chromatin dynamics with approximately 10-fold higher temporal and spatial resolution using the SPT routine for two-photon microscopy described above [42]. Our results showed that chromatin undergoes an apparently confined random motion alternated with short periods of fast-curvilinear motion or jumps (Fig. 7). Statistical analyses of the trajectories showed that the jumps are compatible with active transport. Depletion of cellular ATP pools from cells and slightly lower temperatures resulted in a significant reduction of the number of jumps also supporting a model of short-periods of active transport of chromatin in the nucleus [42].

Cajal bodies

The dynamics of Cajal bodies in live cell nucleus was studied by tracking the motion of bodies labeled with green fluorescent protein [59]. The MSD analysis of the trajectories suggests that the bodies move by random diffusion. However, the diffusion coefficient decreases

~20-folds when the Cajal body is in close proximity to chromatin. After ATP depletion, Cajal bodies explore larger volumes of the nucleus with diffusion coefficients one order higher than in control cells. These results were interpret considering that Cajal bodies present an ATP-dependent interaction with DNA restricting their motion. Treatment of the cells with a transcription inhibitor drug shows a similar shift in the diffusion coefficient values as ATP depletion suggesting that the interaction between Cajal bodies and chromatin may accompany active transcription.

PML bodies

PML bodies dynamics in cell nuclei was studied by following the motion of enhanced yellow fluorescent protein labeled bodies [55]. By qualitative observation of the area explored by the bodies and their velocity in the nucleus, three classes of PML bodies could be distinguished. The fastest PML bodies showed intervals of curvilinear motion. These PML bodies reduced their velocity after ATP depletion or chemical inhibition of myosins, suggesting that nuclear myosin-I is involved in PML bodies's dynamics.

Cell micromechanics

Wirtz and coworkers [50, 88] have developed a method based on particle tracking to measure the mechanics of living cells. In the method, the trajectories of thermally driven microspheres embedded in the cell cytoplasm are measured and the MSD analysis of their trajectories provides a quantitative characterization of the mechanical properties of their microenvironment (for further details, see [50]). In contrast to previous methods to measure cell mechanics, this method has the advantage of not requiring the deformation of the cell [31]. In some cell lines, intrinsic particles such as lipid droplets can be used as probes with the additional advantage that no manipulation to introduce external probes is required [98]. In this case, it is important to establish that the endogenous probes are passively diffusing.

By analyzing enough number of beads, the method allows the mapping of the mechanical properties of different cell regions [88, 89]. This approach is also a powerful tool to measure the mechanical response of cells to certain stimuli. For example, it has been used to study the mechanical properties of fibroblasts during migration [36], the effects of fluid flow on fibroblasts cytoplasm micromechanics [41], and the characteristics of the embryonic cytoplasm in *C. elegans* in early stages of development [15].

Perspectives

Single particle tracking techniques are still at a developing stage. In most of their applications to Cell Biology studies they have demonstrated to be an extremely important tool to understand cellular dynamics. As it has been shown in the few examples mentioned in this review, SPT does not only reveal how a given labeled particle is moving but can give important clues regarding association processes, regulatory mechanisms, intracellular architecture, etc.

Further instrumental and theoretical developments will be fundamental to broaden the applications of these techniques to answer biological issues in vivo. Particularly, the improvement of sensitivity and speed of cameras will allow the study of faster processes, including the motion of small molecules. The development and utilization of techniques to track in three dimensions will generate a better description of dynamics of cellular components not moving within membranes. The extension of SPT to simultaneous tracking of particles labeled with different probes would allow studies of their interaction in cells. Also, quantum dots constitute a big promise since they could be used to label a broader number of particles and track their motion during longer observation periods. Besides the experimental issues, more theoretical work will be required to maximize the information that can be obtained from the trajectories analysis.

References

1. Alberts, B., Johnson, A., Lewis, J., Raff, M., Roberts, K., & Walter, P. (2002). Methods. In *Molecular biology of the cell* (pp. 469–582). New York: Garland Science.
2. Alberts, B., Johnson, A., Lewis, J., Raff, M., Roberts, K., & Walter, P (2002). Cells in their social context. In *Molecular biology of the cell* (pp. 1065–1423). New York: Garland Science.
3. Babcock, H. P., Chen, C., & Zhuang, X. (2004). Using single-particle tracking to study nuclear trafficking of viral genes. *Biophysical Journal, 87*, 2749–2758.
4. Belmont, A. S., & Straight, A. F. (1998). In vivo visualization of chromosomes using lac operator-repressor binding. *Trends in Cell Biology, 8*, 121–124.
5. Belmont, A. S. (2001). Visualizing chromosome dynamics with GFP. *Trends in Cell Biology, 11*, 250–257.
6. Berland, K. M., So, P. T., & Gratton, E. (1995). Two-photon fluorescence correlation spectroscopy: Method and application to the intracellular environment. *Biophysical Journal, 68*, 694–701.
7. Berland, K. M., Jacobson, K. A., Frenche, T., & Rajfur, Z. (2003). Electronic cameras for low-light microscopy. In G. Sluder & D. E. Wolf (Eds.), *Digital microscopy: A second edition of video microscopy* (pp. 103–132). Amsterdam: Elsevier Academic Press.

8. de Brabander, M., Nuydens, R., Ishihara, A., Holifield, B., Jacobson, K., & Geerts, H. (1991). Lateral diffusion and retrograde movements of individual cell surface components on single motile cells observed with Nanovid microscopy. *The Journal of Cell Biology, 112*, 111–124.
9. Bruchez, M. Jr., Moronne, M., Gin, P., Weiss, S., & Alivisatos, A. P. (1998). Semiconductor nanocrystals as fluorescent biological labels. *Science, 281*, 2013–2016.
10. Capps, G. G., Pine, S., Edidin, M., & Zuniga, M. C. (2004). Short class I major histocompatibility complex cytoplasmic tails differing in charge detect arbiters of lateral diffusion in the plasma membrane. *Biophysical Journal, 86*, 2896–2909.
11. Carter, B., Shubeita, G., & Gross, S. (2005). Tracking single particles: A user-friendly quantitative evaluation. *Physical Biology, 2*, 60–72.
12. Cheezum, M. K., Walker, W. F., & Guilford, W. H. (2001). Quantitative comparison of algorithms for tracking single fluorescent particles. *Biophysical Journal, 81*, 2378–2388.
13. Chubb, J. R., Boyle, S., Perry, P., & Bickmore, W. A. (2002). Chromatin motion is constrained by association with nuclear compartments in human cells. *Current Biology, 12*, 439–445.
14. Dahan, M., Levi, S., Luccardini, C., Rostaing, P., Riveau, B., & Triller, A. (2003). Diffusion dynamics of glycine receptors revealed by single-quantum dot tracking. *Science, 302*, 442–445.
15. Daniels, B. R., Masi, B. C., & Wirtz, D. (2006). Probing single-cell micromechanics in vivo: The microrheology of *C. elegans* developing embryos. *Biophysical Journal, 90*, 4712–4719.
16. Deacon, S. W., Serpinskaya, A. S., Vaughan, P. S., Lopez Fanarraga, M., Vernos, I., Vaughan, K. T., & Gelfand, V. I. (2003). Dynactin is required for bidirectional organelle transport. *The Journal of Cell Biology, 160*, 297–301.
17. Digman, M. A., Brown, C. M., Sengupta, P., Wiseman, P. W., Horwitz, A. R., & Gratton, E. (2005). Measuring fast dynamics in solutions and cells with a laser scanning microscope. *Biophysical Journal, 89*, 1317–1327.
18. Dubertret, B., Skourides, P., Norris, D. J., Noireaux, V., Brivanlou, A. H., & Libchaber, A. (2002). In vivo imaging of quantum dots encapsulated in phospholipid micelles. *Science, 298*, 1759–1762.
19. Enderlein, J. (2000). Tracking of fluorescent molecules diffusing within membranes. *Applied Physics B-Lasers and Optics, 71*, 773–777.
20. Feder, T. J., Brust-Mascher, I., Slattery, J. P., Baird, B., & Webb, W. W. (1996). Constrained diffusion or immobile fraction on cell surfaces: a new interpretation. *Biophysical Journal, 70*, 2767–2773.
21. Fujiwara, T., Ritchie, K., Murakoshi, H., Jacobson, K., & Kusumi, A. (2002). Phospholipids undergo hop diffusion in compartmentalized cell membrane. *The Journal of Cell Biology, 157*, 1071–1081.
22. Gao, X., Yang, L., Petros, J. A., Marshall, F. F., Simons, J. W., & Nie, S. (2005). In vivo molecular and cellular imaging with quantum dots. *Current Opinion in Biotechnology, 16*, 63–72.
23. Gasser, S. M. (2002). Visualizing chromatin dynamics in interphase nuclei. *Science, 296*, 1412–1416.
24. Geerts, H., de Brabander, M., & Nuydens, R. (1991). Nanovid microscopy. *Nature, 351*, 765–766.
25. Gelles, J., Schnapp, B. J., & Sheetz, M. P. (1988). Tracking kinesin-driven movements with nanometre-scale precision. *Nature, 331*, 450–453.
26. Gross, S. P., Tuma, M. C., Deacon, S. W., Serpinskaya, A. S., Reilein, A. R., & Gelfand, V. I. (2002). Interactions and regulation of molecular motors in *Xenopus melanophores*. *The Journal of Cell Biology, 156*, 855–865.
27. Gross, S. P., Welte, M. A., Block, S. M., & Wieschaus, E. F. (2002). Coordination of opposite-polarity microtubule motors. *The Journal of Cell Biology, 156*, 715–724.
28. Gross, S. P. (2004). Hither and yon: A review of bi-directional microtubule-based transport. *Physical Biology, 1*, R1–R11.
29. Haughland, R. P. (1998). *Handbook of fluorescent probes and research chemicals*. Eugene, OR: Molecular Probes.
30. Hebert, B., Costantino, S., & Wiseman, P. W. (2005). Spatiotemporal image correlation spectroscopy (STICS) theory, verification, and application to protein velocity mapping in living CHO cells. *Biophysical Journal, 88*, 3601–3614.
31. Heidemann, S. R., & Wirtz, D. (2004). Towards a regional approach to cell mechanics. *Trends in Cell Biology, 14*, 161–166.
32. Heun, P., Laroche, T., Shimada, K., Furrer, P., & Gasser, S. M. (2001). Chromosome dynamics in the yeast interphase nucleus. *Science, 294*, 2181–2186.
33. Hill, D. B., Plaza, M. J., Bonin, K., & Holzwarth, G. (2004). Fast vesicle transport in PC12 neurites: Velocities and forces. *European Journal of Biophysics Journal, 33*, 623–632.
34. Kis-Petikova, K., & Gratton, E. (2004). Distance measurement by circular scanning of the excitation beam in the two-photon microscope. *Microscopy Research and Technique, 63*, 34–49.
35. Klonis, N., Rug, M., Harper, I., Wickham, M., Cowman, A., & Tilley, L. (2002). Fluorescence photobleaching analysis for the study of cellular dynamics. *European Journal of Biophysics Journal, 31*, 36–51.
36. Kole, T. P., Tseng, Y., Jiang, I., Katz, J. L., & Wirtz, D. (2005). Intracellular mechanics of migrating fibroblasts. *Molecular Biology of the Cell, 16*, 328–338.
37. Kuno, M., Fromm, D. P., Hamann, H. F., Gallagher, A., & Nesbitt, D. J. (2000). Nonexponential ''blinking'' kinetics of single CdSe quantum dots: A universal power law behavior. *The Journal of Chemical Physics, 112*, 3117–3120.
38. Kural, C., Kim, H., Syed, S., Goshima, G., Gelfand, V. I., & Selvin, P. R. (2005). Kinesin and dynein move a peroxisome in vivo: A tug-of-war or coordinated movement? *Science, 308*, 1469–1472.
39. Kusumi, A., Nakada, C., Ritchie, K., Murase, K., Suzuki, K., Murakoshi, H., Kasai, R. S., Kondo, J., & Fujiwara, T. (2005). Paradigm shift of the plasma membrane concept from the two-dimensional continuum fluid to the partitioned fluid: High-speed single-molecule tracking of membrane molecules. *Annual Review of Biophysics and Biomolecular Structure, 34*, 351–378.
40. Lakadamyali, M., Rust, M. J., Babcock, H. P., & Zhuang, X. (2003). Visualizing infection of individual influenza viruses. *Proceedings of the National Academy of Sciences of the United States of America, 100*, 9280–9285.
41. Lee, J. S., Panorchan, P., Hale, C. M., Khatau, S. B., Kole, T. P., Tseng, Y., & Wirtz, D. (2006). Ballistic intracellular nanorheology reveals ROCK-hard cytoplasmic stiffening response to fluid Flow. *Journal of Cell Science*, 1760–1768.
42. Levi, V., Ruan, Q., Plutz, M., Belmont, A. S., & Gratton, E. (2005). Chromatin dynamics in interphase cells revealed by tracking in a two-photon excitation microscope. *Biophysical Journal, 89*, 4275–4285.
43. Levi, V., Ruan, Q., & Gratton, E. (2005). 3-D particle tracking in a two-photon microscope: application to the study of molecular dynamics in cells. *Biophysical Journal, 88*, 2919–2928.

44. Levi, V., Serpinskaya, A. S., Gratton, E., & Gelfand, V. (2006). Organelle transport along microtubules in *Xenopus melanophores*: evidence for cooperation between multiple motors. *Biophysical Journal, 90*, 318–327.
45. Levi, V., Gelfand, V. I., Serpinskaya, A. S., & Gratton, E. (2006). Melanosomes transported by Myosin-V in *Xenopus melanophores* perform slow 35 nm steps. *Biophysical Journal, 90*, L7–L9.
46. Lommerse, P. H., Spaink, H. P., & Schmidt, T. (2004). In vivo plasma membrane organization: results of biophysical approaches. *Biochimica et Biophysica Acta, 1664*, 119–131.
47. Lommerse, P. H., Snaar-Jagalska, B. E., Spaink, H. P., & Schmidt, T. (2005). Single-molecule diffusion measurements of H-Ras at the plasma membrane of live cells reveal microdomain localization upon activation. *Journal of Cell Science, 118*, 1799–1809.
48. Ma, S., & Chisholm, R. L. (2002). Cytoplasmic dynein-associated structures move bidirectionally in vivo. *Journal of Cell Science, 115*, 1453–1460.
49. Marshall, W. F., Straight, A., Marko, J. F., Swedlow, J., Dernburg, A., Belmont, A., Murray, A. W., Agard, D. A., & Sedat, J. W. (1997). Interphase chromosomes undergo constrained diffusional motion in living cells. *Current Biology, 7*, 930–939.
50. Mason, T. G., Ganesan, K., van Zanten, J. H., Wirtz, D., & Kuo, S. C. (1997). Particle tracking microrheology of complex fluids. *Physical Review Letters, 79*, 3282–3285.
51. Meier, J., Vannier, C., Serge, A., Triller, A., & Choquet, D. (2001). Fast and reversible trapping of surface glycine receptors by gephyrin. *Nature Neuroscience, 4*, 253–260.
52. Michalet, X., Pinaud, F. F., Bentolila, L. A., Tsay, J. M., Doose, S., Li, J. J., Sundaresan, G., Wu, A. M., Gambhir, S. S., & Weiss, S. (2005). Quantum dots for live cells, in vivo imaging, and diagnostics. *Science, 307*, 538–544.
53. Misteli, T. (2005). Concepts in nuclear architecture. *Bioessays, 27*, 477–487.
54. Murase, K., Fujiwara, T., Umemura, Y., Suzuki, K., Iino, R., Yamashita, H., Saito, M., Murakoshi, H., Ritchie, K., & Kusumi, A. (2004). Ultrafine membrane compartments for molecular diffusion as revealed by single molecule techniques. *Biophysical Journal, 86*, 4075–4093.
55. Muratani, M., Gerlich, D., Janicki, S. M., Gebhard, M., Eils, R., & Spector, D. L. (2002). Metabolic-energy-dependent movement of PML bodies within the mammalian cell nucleus. *Nature Cell Biology, 4*, 106–110.
56. On-chip multiplication gain. (2002). Technical Note 14. In. Trenton, NJ: Roper Scientific.
57. Oshiro, M., & Moomaw, B. (2003). Cooled vs. intensified vs. electron bombardment CCD cameras–applications and relative advantages. In G. Sluder & D. E. Wolf (Eds.), *Digital microscopy: A second edition of video microscopy* (pp. 133–156). Amsterdam: Elsevier Academic Press.
58. Piston, D. (1996). Two-photon excitation microscopy. In X. Wang & B. Herman (Eds.), *Fluorescence imaging spectroscopy and microscopy* (pp. 253–272). New York: John Wiley & Sons.
59. Platani, M., Goldberg, I., Lamond, A. I., & Swedlow, J. R. (2002). Cajal body dynamics and association with chromatin are ATP-dependent. *Nature Cell Biology, 4*, 502–508.
60. Qian, H., Sheetz, M. P., & Elson, E. L. (1991). Single particle tracking. Analysis of diffusion and flow in two-dimensional systems. *Biophysical Journal, 60*, 910–921.
61. Reits, E. A., & Neefjes, J. J. (2001). From fixed to FRAP: measuring protein mobility and activity in living cells. *Nature Cell Biology, 3*, E145–E147.
62. Ritchie, K., Iino, R., Fujiwara, T., Murase, K., & Kusumi, A. (2003). The fence and picket structure of the plasma membrane of live cells as revealed by single molecule techniques (Review). *Molecular Membrane Biology, 20*, 13–18.
63. Rogers, S. L., Tint, I. S., & Gelfand, V. I. (1998). In vitro motility assay for melanophore pigment organelles. *Methods in Enzymology, 298*, 361–372.
64. Ruan, Q., Cheng, M. A., Levi, M., Gratton, E., & Mantulin, W. W. (2004). Spatial-temporal studies of membrane dynamics: scanning fluorescence correlation spectroscopy (SFCS). *Biophysical Journal, 87*, 1260–1267.
65. Sako, Y., & Kusumi, A. (1994). Compartmentalized structure of the plasma membrane for receptor movements as revealed by a nanometer-level motion analysis. *The Journal of Cell Biology, 125*, 1251–1264.
66. Sako, Y., Minoghchi, S., & Yanagida, T. (2000). Single-molecule imaging of EGFR signalling on the surface of living cells. *Nature Cell Biology, 2*, 168–172.
67. Sako, Y., & Uyemura, T. (2002). Total internal reflection fluorescence microscopy for single-molecule imaging in living cells. *Cell Structure and Function, 27*, 357–365.
68. Sanchez, S. A., & Gratton, E. (2005). Lipid–protein interactions revealed by two-photon microscopy and fluorescence correlation spectroscopy. *Accounts of Chemical Research, 38*, 469–477.
69. Saxton, M. J., & Jacobson, K. (1997). Single-particle tracking: Applications to membrane dynamics. *Annual Review of Biophysics and Biomolecular Structure, 26*, 373–399.
70. Saxton, M. J. (1994). Anomalous diffusion due to obstacles: A Monte Carlo study. *Biophysical Journal, 66*, 394–401.
71. Saxton, M. J. (1994). Single-particle tracking: Models of directed transport. *Biophysical Journal, 67*, 2110–2119.
72. Saxton, M. J. (1997). Single-particle tracking: the distribution of diffusion coefficients. *Biophysical Journal, 72*, 1744–1753.
73. Saxton, M. J. (1996). Anomalous diffusion due to binding: A Monte Carlo study. *Biophysical Journal, 70*, 1250–1262.
74. Saxton, M. J. (1993). Lateral diffusion in an archipelago. Single-particle diffusion. *Biophysical Journal, 64*, 1766–1780.
75. Saxton, M. J. (1995). Single-particle tracking: Effects of corrals. *Biophysical Journal, 69*, 389–398.
76. Schneckenburger, H. (2005). Total internal reflection fluorescence microscopy: technical innovations and novel applications. *Current Opinion in Biotechnology, 16*, 13–18.
77. Sheetz, M. P., Turney, S., Qian, H., & Elson, E. L. (1989). Nanometre-level analysis demonstrates that lipid flow does not drive membrane glycoprotein movements. *Nature, 340*, 284–288.
78. Simson, R., Yang, B., Moore, S. E., Doherty, P., Walsh, F. S., & Jacobson, K. A. (1998). Structural mosaicism on the submicron scale in the plasma membrane. *Biophysical Journal, 74*, 297–308.
79. Singer, S. J., & Nicolson, G. L. (1972). The fluid mosaic model of the structure of cell membranes. *Science, 175*, 720–731.
80. So, P. T., Dong, C. Y., Masters, B. R., & Berland, K. M. (2000). Two-photon excitation fluorescence microscopy. *Annual Review of Biomedical Engineering, 2*, 399–429.
81. Sodeik B. (2000). Mechanisms of viral transport in the cytoplasm. *Trends in Microbiology, 8,* 465–472.
82. Spring, K. R. (2003). Cameras for digital microscopy. In G. Sluder & D. E. Wolf (Eds.), *Digital microscopy: A second edition of video microscopy* (pp. 87–132). Amsterdam: Elsevier Academic Press.

83. Stephens, D. J., & Allan, V. J. (2003). Light microscopy techniques for live cell imaging. *Science, 300*, 82–86.
84. Syed, S., Snyder, G. E., Franzini-Armstrong, C., Selvin, P. R., & Goldman, Y. E. (2006). Adaptability of myosin V studied by simultaneous detection of position and orientation. *The Embo Journal, 25*, 1795–1803.
85. Thompson, R. E., Larson, D. R., & Webb, W. W. (2002). Precise nanometer localization analysis for individual fluorescent probes. *Biophysical Journal, 82*, 2775–2783.
86. Tomishige, M., Sako, Y., & Kusumi, A. (1998). Regulation mechanism of the lateral diffusion of band 3 in erythrocyte membranes by the membrane skeleton. *The Journal of Cell Biology, 142*, 989–1000.
87. Toprak, E., Enderlein, J., Syed, S., McKinney, S. A., Petschek, R. G., Ha, T., Goldman, Y. E., & Selvin, P. R. (2006). Defocused orientation and position imaging (DOPI) of myosin V. *Proceedings of the National Academy of Sciences of the United States of America, 103*, 6495–6499.
88. Tseng, Y., Kole, T. P., & Wirtz, D. (2002). Micromechanical mapping of live cells by multiple-particle-tracking microrheology. *Biophysical Journal, 83*, 3162–3176.
89. Tseng, Y., Lee, J. S., Kole, T. P., Jiang, I., & Wirtz, D. (2004). Micro-organization and visco-elasticity of the interphase nucleus revealed by particle nanotracking. *Journal of Cell Science, 117*, 2159–2167.
90. Tsien, R. Y. (1998). The green fluorescent protein. *Annual Review of Biochemistry, 67*, 509–544.
91. Tumbar, T., & Belmont, A. S. (2001). Interphase movements of a DNA chromosome region modulated by VP16 transcriptional activator. *Nature Cell Biology, 3*, 134–139.
92. Vale, R. D. (2003). The molecular motor toolbox for intracellular transport. *Cell, 112*, 467–480.
93. Vazquez, J., Belmont, A. S., & Sedat, J. W. (2001). Multiple regimes of constrained chromosome motion are regulated in the interphase Drosophila nucleus. *Current Biology, 11*, 1227–1239.
94. Warshaw, D. M., Kennedy, G. G., Work, S. S., Krementsova, E. B., Beck, S., & Trybus, K. M. (2005). Differential labeling of myosin V heads with quantum dots allows direct visualization of hand-over-hand processivity. *Biophysical Journal, 88*, L30–L32.
95. Wazawa, T., & Ueda, M. (2005). Total internal reflection fluorescence microscopy in single molecule nanobioscience. *Advances in Biochemical Engineering/Biotechnology, 95*, 77–106.
96. Welte, M. A., Gross, S. P., Postner, M., Block, S. M., & Wieschaus, E. F. (1998). Developmental regulation of vesicle transport in Drosophila embryos: Forces and kinetics. *Cell, 92*, 547–557.
97. Welte, M. A. (2004). Bidirectional transport along microtubules. *Current Biology, 14*, R525–R537.
98. Yamada, S., Wirtz, D., & Kuo, S. C. (2000). Mechanics of living cells measured by laser tracking microrheology. *Biophysical Journal, 78*, 1736–1747.
99. Yildiz, A., Forkey, J. N., McKinney, S. A., Ha, T., Goldman, Y. E., & Selvin, P. R. (2003). Myosin V walks hand-over-hand: single fluorophore imaging with 1.5-nm localization. *Science, 300*, 2061–2065.
100. Yildiz, A., Park, H., Safer, D., Yang, Z., Chen, L. Q., Selvin, P. R., & Sweeney, H. L. (2004). Myosin VI steps via a hand-over-hand mechanism with its lever arm undergoing fluctuations when attached to actin. *The Journal of Biological Chemistry, 279*, 37223–37226.
101. Yildiz, A., Tomishige, M., Vale, R. D., & Selvin, P. R. (2004). Kinesin walks hand-over-hand. *Science, 303*, 676–678.